12A.6 RADAR CLIMATOLOGY OF HONG KONG AND ITS APPLICATION TO LANDFALLING TROPICAL CYCLONE RAINFALL ESTIMATION

Linus H.Y. Yeung*[1], S.T. Chan[1] and P.W. Cheng[2]
[1] Hong Kong Observatory, Hong Kong, China
[2] City University of Hong Kong, Hong Kong, China

1. INTRODUCTION

Radar climatology has been studied at many places over the world (Kuo & Orville 1973; James *et al*. 2004; Overeem *et al*. 2009; Chang *et al*. 2009; Weckwerth *et al*. 2011) for various purposes. In Hong Kong, the first radar climatological study was performed by Cheng and Kwong (1973), who analyzed the observations from a Plessey Type 43S Radar (10 cm wavelength) to study the diurnal, daily and monthly variations of radar echo coverage in Hong Kong during the period 1967-1969. One of the common themes in studying radar climatology is the effect of orography on precipitation. Recently, there are also case studies (Yu & Cheng 2008; Smith *et al*. 2009) using radar observations to investigate the orographic enhancement of precipitation due to typhoon or hurricane.

Hong Kong is small in area but complex in topography. As shown in Fig. 1 there are numerous mountain ranges with significant altitudes scattered all over the territory. The highest peak is 957 m above mean sea level located at Tai Mo Shan (labeled TMS in Fig. 1(a)). From the annual mean rainfall analysis over Hong Kong (Fig. 1(b) refers), it is evident that the local maxima are associated with the terrain peaks. The orographic effect is more prominent under strongly forced situations, say when a TC approaches the south China coast and brings high winds to Hong Kong. Depending on its motion track and intensity of an approaching TC, different high wind regimes can be resulted. Orographic lift, and therefore rainfall enhancement, is expected to occur over those mountain ranges that are blocking the prevailing air flow.

In this study, radar reflectivity climatology of Hong Kong will be computed based on a representative set of historical tropical cyclone cases to be described in Section 2. The climatological distributions of radar reflectivity will be analyzed according to wind regimes and the results presented in Section 3. Compared in Section 4 are the corresponding climatological rainfall distributions as analyzed from raingauge data. Section 5 will describe the conversion from radar reflectivity to rainfall rates used in this study. The characteristics of the observed enhancement patterns are discussed in Section 6. Section 7 will conclude the study and outline the ways forward on applications to rainfall nowcasting.

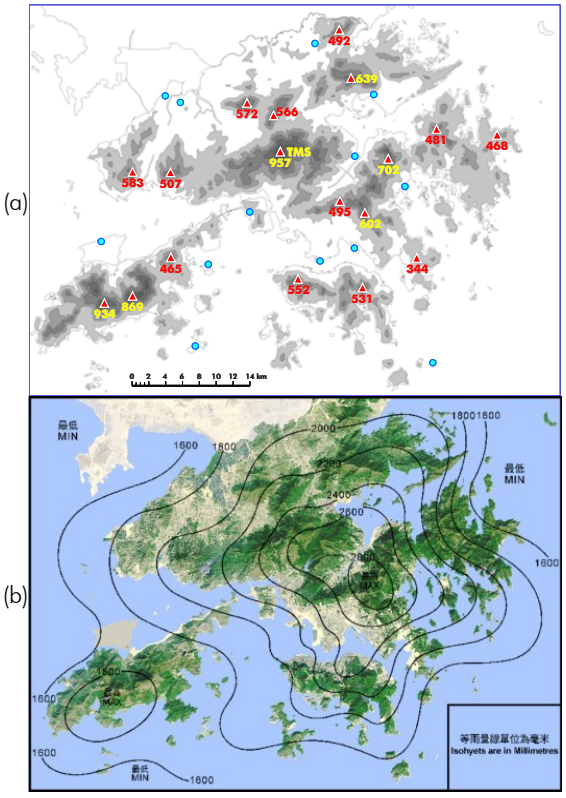

Fig. 1 Terrain map (a) and mean annual rainfall map (b) of Hong Kong. Topography is shown as shaded contours at 125-m intervals. Major peaks are marked by red triangles with altitudes annotated in unit of metre. The anemometer stations used in this study are marked by blue circles. The rainfall distribution refers to the period 1971-2000. The highest isohyet is 2,800 mm.

2. DATA SETS

A list of 36 tropical cyclone (TC) cases during 1999-2010 was selected for the present study. This includes all the TCs that came within a proximity range of 256 km from the Hong Kong Observatory's TMS weather radar since its operation in 1999. The time duration that a TC spent within this proximity (referred to as "proximity period" for notational convenience) ranges from a few hours to over two days, with an average about 20 hours. The maximum local winds brought about by these TCs vary from strong to hurricane force with directions spanning throughout the compass. The wind rose diagram in Fig. 2 shows the frequency distribution of local winds calculated from the 36 TCs under study.

*Corresponding author address: Linus H.Y. Yeung, Hong Kong Observatory, 134A, Nathan Road, Kowloon, Hong Kong, China; e-mail: hyyeung@hko.gov.hk

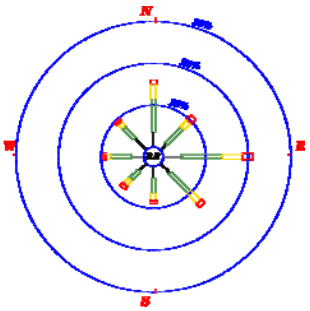

Fig. 2 Wind rose plotted for the TC cases within Hong Kong's proximity range during 1999-2010. The black, green, yellow and red lines refer to wind-force ranges 1-2, 3-4, 5-6 and over 6 in Beaufort scale respectively. The number in the middle indicates the percentage of calm and variable winds. The percentages of the four wind-force ranges are 23.6, 44.8, 19.8 and 8.5% respectively.

The radar reflectivity data came from by the TMS radar, which is a S-band Doppler weather radar located at Tai Mo Shan ("TMS" in Fig. 1 refers) in Hong Kong. The volume scan is performed once every 6 minutes. Basic quality control is applied to the raw radar data to remove clutters. The reflectivity data at a constant altitude of 2 km above sea level were used to compute the climatological distributions. To allow direct comparison with rain gauge observations, the reflectivity was converted to rainfall rates using the Z-R relation, $Z = a R^b$. The values of the parameters *a* and *b* are 228.82 and 1.33 respectively, the determination of which will be explained in Section 5 below. Discounting the missing or corrupted data, the radar scans available cover about 90% of the total proximity period of all TCs.

The rainfall observations were collected from the automatic rain gauge network in Hong Kong. Currently, there are 157 rain gauges available, covering a total land area of about 1,100 km^2. The rain gauges have a resolution of 0.5 mm and the data are reported at 5-minute intervals. To allow direct comparison with the rainfall rates deduced from the mean radar reflectivity fields, we took the 5-minute rain-gauge accumulations as an estimate for rainfall rate and multiplied the values by 12 to cast it in unit of mm/h. The required climatological distributions were then obtained and gridded to the same grid as for the radar (252x217 at 0.267 km spacing) by interpolation using the Kriging analysis technique (Yeung *et al*. 2011).

3. TC WIND REGIMES & MEAN REFLECTIVITY

Depending on the track and intensity of an approaching TC, the local wind direction and speed may change significantly as it gets close to or even passes over a place. Hilly terrain in general will also affect the local wind strength. As shown in Fig. 2, the percentage of high winds (force 6 or above) is climatologically slim even during proximity periods. It follows that a simple average over the entire data set may not be able to delineate clearly the full effects of orographic enhancement. To this end, the observation data were stratified into eight basic wind groups according to the directions on a 8-point compass. As hinted by Fig. 2, some wind directions are naturally preferred to the others and the wind groups were combined further into 4 regimes, namely north to northeasterly (denoted N+NE), east to southeasterly (denoted E+SE), south to southwesterly (denoted S+SW) and west to northwesterly (denoted W+NW). With these combinations, the statistical significance in each regime can also be enhanced. Here, the wind directions for data grouping refer to the average wind directions determined by taking the vector mean of the 10-minute mean winds reported at 13 representative anemometer stations in Hong Kong. These anemometers are located near sea level (blue circles on Fig. 1) and are used as reference stations in support of the tropical cyclone warning system in Hong Kong.

The mean reflectivity fields calculated for the 4 wind regimes are shown in Fig. 3 below. As explained in Section 2, the data shown in the plots are converted to rainfall rate in unit of mm/h for direct comparison with those derived from rain gauge data. It is apparent that high winds from different directions produce different degrees of enhancement at different locations over the territory. In general, the reflectivity maxima seen in a wind regime can be correlated with the mountain ranges that block the corresponding prevailing flows. While the maximum shown in the upper right corner of Fig. 3 (c) for the S+SW directions is considered not representative (samples least abundant in the S+SW directions and effect averaged out in the mean field (e) over all regimes), the off-slope maximum near the centre of Fig. 3 (b) for N+NE is believed to be a genuine feature and discussed in Section 6 below. There exist two blank sectors common to all plots in the southeast quadrant due to the blockage by obstructions close to the radar at TMS.

4. TC RAINFALL CLIMATOLOGY

Plotted in Fig. 4(a)-(d) are the mean rainfall-rate fields corresponding to the 4 wind regimes shown in Fig. 3. Fig. 4(e) shows the mean rainfall rate over all wind regimes. The maximum is located over the TMS and different from that of the long-term climatological annual rainfall distribution shown in Fig. 1(b). Similar to the mean reflectivity, the maxima of the mean rainfall rates in individual wind regimes are found over different mountain ranges. However, several differences are noted. Firstly, the locations of the maxima are slightly offset from those seen in the mean reflectivity fields. One possible reason may be related to the significant advection effect by TC high winds on the rain drops during their fall from 2 km altitude (the level at which reflectivity were sampled) to the ground (where the rainfall rates were estimated). Secondly, the prominent enhancement seen in Fig. 3(d) over the eastern mountains under the E+SE regime is not obvious in Fig. 4(d). Further investigation will be needed to explain the difference. Thirdly, enhancements on the southern slopes of the largest island (called Lantau) in the southwestern part of Hong Kong are not prominent when compared with their mean reflectivity counterparts. This is possibly related to the scarcity of rain gauges over there.

5. REFLECTIVITY-RAINFALL CONVERSION

The Hong Kong Observatory operates a rainfall nowcasting system known as SWIRLS (Short-range Warning of Intense Rainstorms in Localized Systems; Li & Lai 2004; Yeung *et al*. 2009) for predicting the rainfall dis-

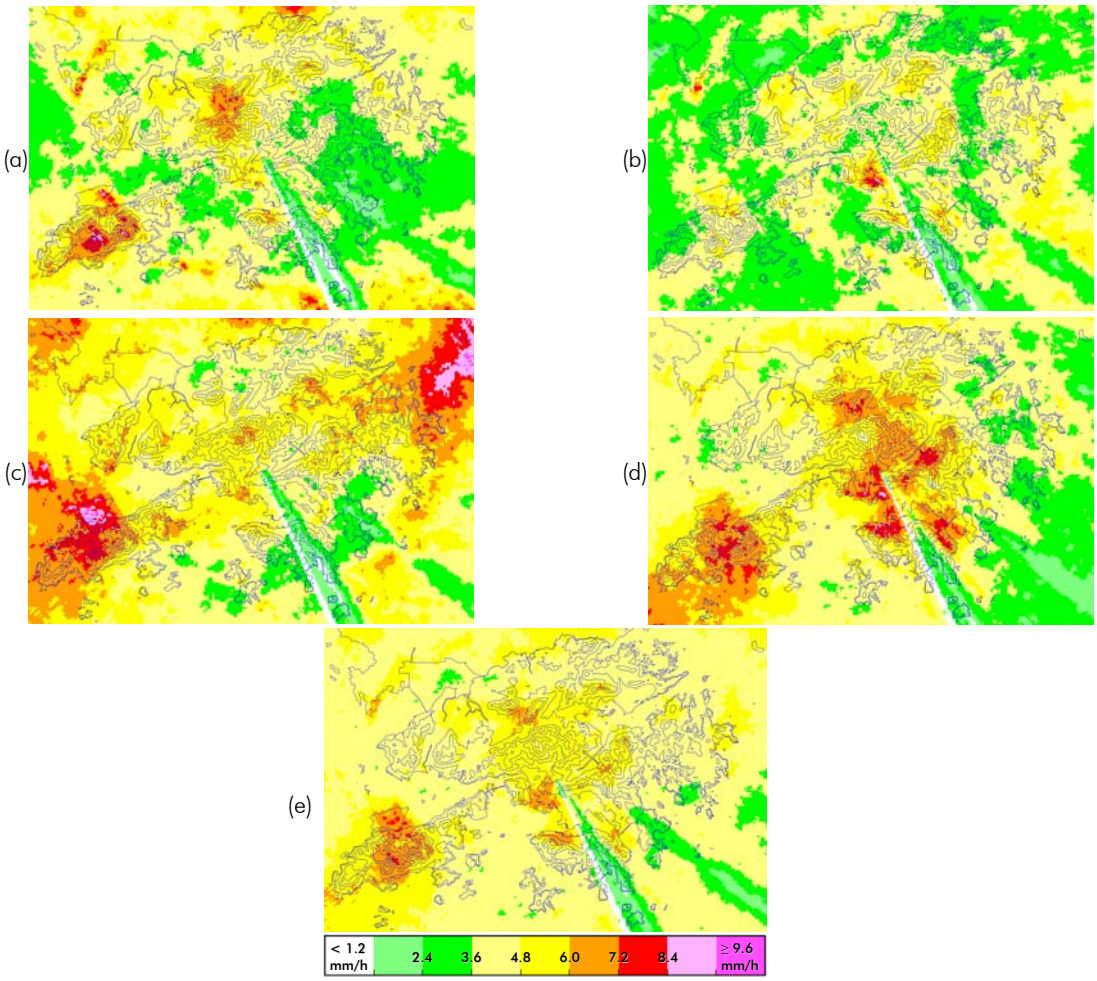

Fig. 3 Mean reflectivity fields converted to rainfall rates for 4 wind regimes: (a) W+NW; (b) N+NE; (c) S+SW; (d) E+SE. Shown in (e) is the mean field over all regimes. The two weak-echo sectors common to all plots are due to the blockage by an obstructions close to the radar at TMS.

tribution over Hong Kong and nearby regions based on the extrapolation of radar reflectivity. One of the crucial steps is the estimation of rainfall rate from radar reflectivity through the use of the Z-R relation. In SWIRLS, the two parameters *a* and *b* are calibrated dynamically using real-time rain-gauge data (Li & Lai 2004). For a new rainfall event or when data are insufficient for calibration, a default set of values determined from historical reflectivity and rain gauge data will be used. Currently, the default setting is: $a = 118.2$ and $b = 1.52$. Except for extreme rainfall situations, these default parameters can represent the local rainfall climate satisfactorily and the dynamic calibration approach can further improve the estimation in real-time. However, the above operational procedure does not distinguish between flow regimes and are applied to both TC & non–TC cases. With the availability of a large set of TC rainfall data, we re-analyze the Z-R parameters for different TC cases.

Table I summarized the Z-R parameters calculated for the five TCs that produced the most serious rainstorms (with hourly rainfall exceeding 50 mm) in Hong Kong during their passages. Coincidentally, these five rainstorms are associated with different local wind regimes. While *a* ranges from 107.2 to 274.6, *b* ranges from 1.35 to 1.55. Among these five cases, the rainstorm brought about by Typhoon Neoguri was most intense and the corresponding *b* value is the smallest (1.35). In other less severe TC rainstorms (not shown), *b* mainly lies between 1.30 and 1.52, i.e. less than the default value of *b*. When all the TC data were pooled together for re-analysis, a Z-R setting with $a = 228.82$ and $b = 1.33$ was obtained. These values shall be more representative of the TC rainfall climatology in Hong Kong and therefore can serve as a better default setting for TC situations.

Table I – Z-R parameters for the five TCs that produce serious rainstorms in Hong Kong during their passages.

TC			Wind Regime	Z-R Parameter	
Name	I.D.	Intensity	(rainstorm)	*a*	*b*
York	9915	Typhoon	N to NE	107.25	1.55
Unnamed storm in Sep 2006	-	Tropical Depression	E	231.05	1.40
Neoguri	0801	Typhoon	S to SE	274.66	1.35
Fengshen	0806	Typhoon	SW	250.16	1.36
Molave	0906	Typhoon	W to SW	267.67	1.52

6. DISCUSSION

The mean fields shown in Fig. 3 and Fig. 4 indicated

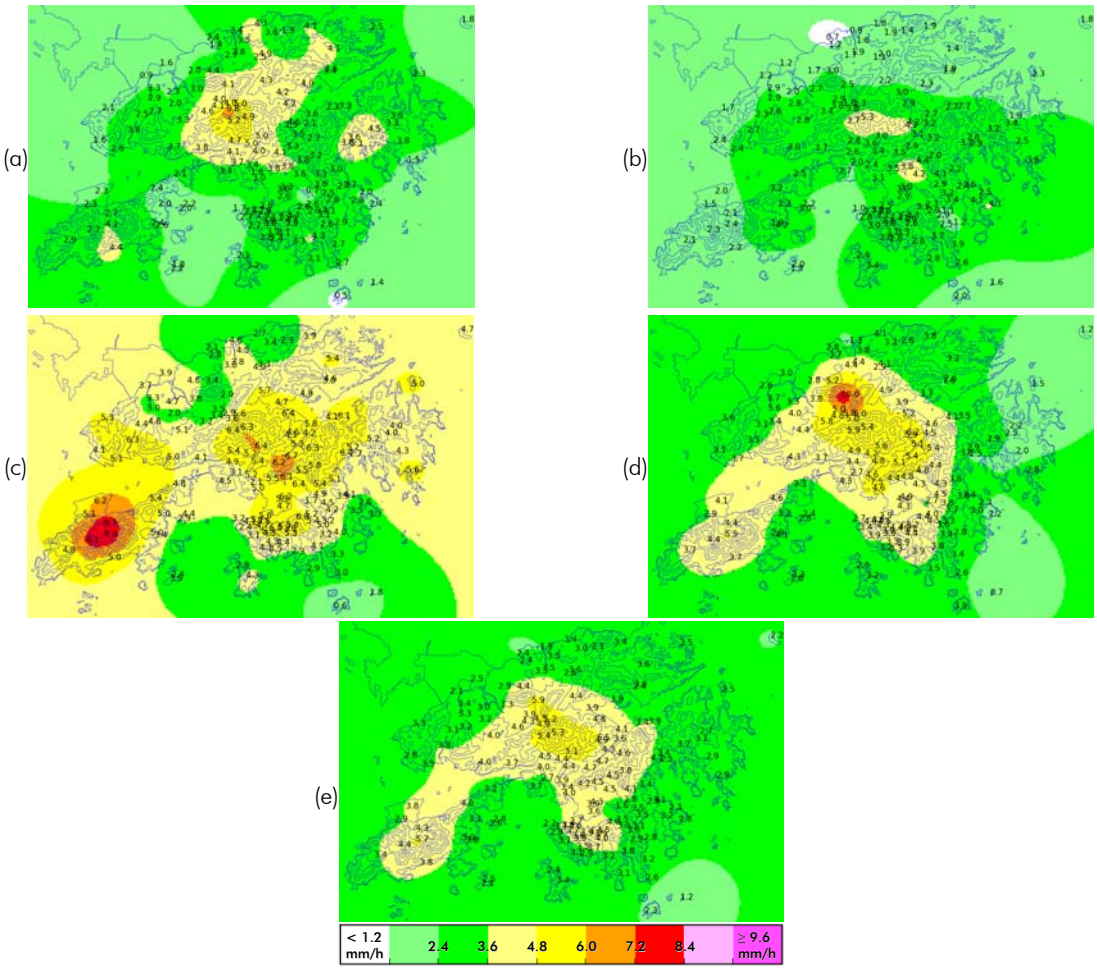

Fig. 4 Same as Fig. 3, except that the plot element is the mean rainfall rate derived from the 5-minute rain gauge rainfall data. Colour shadings represent isohyets analyzed using the Kriging technique.

that the local orography in Hong Kong can enhance rainfall either over the windward slope or the lee side of a mountain range during TC high wind situations. In such wind regimes, the Froude number is expected to be relatively large. The precipitation enhancement over windward slope in such situations has been well discussed in the literature (Hamuro *et al*. 1969; Lin *et al*. 2001; Wu *et al*. 2002; Yu & Cheng 2008). As for the enhancement over the lee side of a mountain, the mechanism is less clear. As pointed out by Yu and Cheng (2008), mountain waves are insignificant as buoyancy force will be rather small in a saturated and convectively neutral environment often found in TC flow regimes. As such, the off-slope maxima seen in Fig. 3 are believed not to be directly resulted from standing lee waves.

Here, we noted that the mountain ranges in Hong Kong orient mainly SW-NE and are mostly less than 10 km in width across the ridge axis. When winds come from the SW or NE, a mountain range in general will open up a gentler slope to the oncoming flows. In contrast, the same mountain range will present a steeper and wider barrier if winds come from the orthogonal directions. According to the study by Yu and Cheng (2008) on orographic precipitation enhancement associated with Typhoon Xangsane (2000), as low-level oncoming flow increases, precipitation tends to shift downstream, becoming deeper and wider in extent, as well as stronger in intensity. Shorter and smaller mountains will be more effective than their taller and bigger counterparts. Whether such case study results can be applied to explain the observed enhancement patterns in Hong Kong will require a further in-depth analysis and is beyond the scope of this paper.

As pointed out in Section 3, the number of data samples in some wind directions or regimes is still not large enough to average out the effect of individual TC cases in the context of climatology. When more samples are collected for each wind regime in Hong Kong in the future, it will be interesting to investigate how the rainfall maxima will change according to different wind speeds in a given regime. Sufficient samples will also allow the climatological Z-R relations to be further analyzed according to wind regimes and the refined results be applied to rainfall analysis in nowcasting more effectively.

In terms of application to quantitative precipitation forecast (QPF), the mean rainfall rate fields shown in Fig. 3 and Fig. 4 will require further processing before they can be applied quantitatively due to the difference in their absolute intensities, the locations of the maxima and the representativeness of the observation methods. One possible way is to normalize the two sets of fields by their corresponding spatial means calculated over the analysis

grid covering Hong Kong for all wind regimes. The resulting fields will indicate the degree of enhancement, independent of the absolute rainfall rate. Given the blocked sectors in radar and the generally coarser resolution of the raingauge network as mentioned in Section 3 and 4, one further step deemed necessary is to combine the two enhancement maps of a wind regime into one by taking the maximum of the two enhancement factors at every grid point.

7. CONCLUDING REMARKS

Based on a set of 36 proximate TCs since 1999, the mean rainfall-rate fields derived from radar reflectivity and raingauge data of Hong Kong were computed and analyzed according to wind regimes. Orographic enhancement characteristics of the regimes were observed and discussed. When the enhancement maps as discussed in Section 6 become available, they can provide an objective basis for adjusting the rainfall-rate field required in rainfall nowcasting according to wind regimes. The new Z-R relation obtained from the proximate TC data sets can also provide a better default setting for converting radar reflectivity to rainfall rates representative of the local TC rainfall climate. Further investigations on orographic enhancement according to wind speed and Z-R relation for individual wind regimes will be pursued in the future when more proximate TC data become available.

Looking further ahead, application to QPF may be extended beyond the nowcasting range if local wind regimes can be forecasted accurately in the, say short or medium range. This in turn translates to an accurate forecast TC track *a priori*. Given the significant forecast uncertainty in TC track and coarse representation of orography by currently available global numerical weather prediction models, the forecast surface winds for a hilly place close to a TC may not be accurate enough for the climatological findings in this study to be applied directly. As an alternative approach, stratification of the rainfall climatology and orographic enhancement according to TC track regimes may be pursued.

ACKNOWLEDGEMENT

The authors are grateful for Mr T.L. Cheng for his assistance in performing the Z-R analysis.

REFERENCE

Chang, P. L., P. F. Lin, B. J. D. Jou, J. Zhang, 2009: An Application of Reflectivity Climatology in Constructing Radar Hybrid Scans over Complex Terrain. *J. Atmos. Oceanic Technol.*, **26**, 1315–1327.

Cheng, T.T. and W.P. Kwong, 1973: Radar climatology of Hong Kong for the years 1967–1969. *Hong Kong Observatory Technical Note*, No.**34**.

Hamuro, M. and Coauthors, 1969: Precipitation bands of Typhoon Vera in 1959 (Part 1). *J. Meteor. Soc. Japan*, **47**, 298–308.

James, C. N., A. Z. Prescott and R. A. Houze, 2004: A Radar Observations of Orographic Precipitation Over Coastal Northern California. *The 11th AMS Conference on Mountain Meteorology and the Annual Mesoscale Alpine Program (MAP)*, Bartlett, New Hampshire, USA, 21-25 June 2004.

Kuo, J.T. and H.D. Orville, 1973: A Radar Climatology of Summertime Convective Clouds in the Black Hills. *J. Appl. Met.*, **12**, 359-368.

Li, P.W. and E.S.T. Lai, 2004: Short-range quantitative precipitation forecasting in Hong Kong. *J. Hydrology*, **288**, 189-209.

Lin, Y.-L., S. Chiao, T.-A. Wang, M. L. Kaplan and R. P. Weglarz, 2001: Some common ingredients for heavy orographic rainfall. *Wea. Forecasting*, **16**, 633–660.

Overeem, A., I. Holleman, A. Buishand, 2009: Derivation of a 10-Year Radar-Based Climatology of Rainfall. *J. Appl. Meteor. Climatol.*, **48**, 1448–1463;

Smith, R.B., P. Schafer, D. Kirshbaum, E. Regina, 2009: Orographic Enhancement of Precipitation inside Hurricane Dean. *J. Hydromet.*, **10**, 820-831.

Weckwerth, T. M., J. W. Wilson, M. Hagen, T. J. Emerson1, J. O. Pinto, D. L. Rife and L. Grebe, 2011: Radar climatology of the COPS region. *Q.J. Roy. Met. Soc.*, **137**, 31–41.

Wu, C.-C., T.-H. Yen, Y.-H. Kuo and W. Wang, 2002: Rainfall simulation associated with Typhoon Herb (1996) near Taiwan. Part I: The topographic effect. *Wea. Forecasting*, **17**, 1001–1015.

Yeung, Linus H.Y., W.K. Wong, Philip K.Y. Chan and Edwin S.T. Lai, 2009: Applications of the Hong Kong Observatory nowcasting system SWIRLS-2 in support of the 2008 Beijing Olympic Games. *WMO Symposium on Nowcasting*, Whistler, B.C., Canada, 30 Aug-4 Sep 2009.

Yeung, H.Y., C. Man, S.T. Chan and A. Seed, 2011: Application of Radar-Raingauge Co-Kriging to Improve QPE and Quality Control of Real-time Rainfall Data. *Proceedings of the International Symposium on Weather Radar and Hydrology*, Exeter, U.K., 18-21 April 2011.

Yu, C.K. and L.W. Cheng, 2008: Radar Observations of Intense Orographic Precipitation Associated with Typhoon Xangsane (2000). *Mon. Wea. Rev.*, **136**, 497-521.